

$|E_z|$. The size of each image plane displayed is $700 \times 700 \text{ nm}^2$ ($140(x) \times 140(y)$ cells) in front of the probe. The x-component of electric fields form a four petals field pattern distributed symmetrically along the rim of the tip apex much smaller than the y-, z-component of electric fields. The z-component of electric fields form a two petals field pattern distributed symmetrically along the rim of the tip apex, is also smaller than y-component of electric fields, an intriguing enhancement occurs at the rim of the tip apex. Both $|E_x|$ and $|E_z|$ decay rapidly as the distance away from the probe increases. The y-component of electric fields leads to propagation mainly in forward direction along the optical axial and possess the total field distribution mostly emerging from the tip. The depolarization phenomenon of components of electric fields is the near-field effect. Recall that under the weak scattering probe (Rayleigh particle), where the interaction of the tip with the electromagnetic field near the sample surface is approximately negligible. The weak scatterer approximation the strongest intensities are found near the center of the tip apex. As shown in Figs. 4(c),(d), obviously, for this non-coated probe, s-polarization is predominate for surface digging. The p-polarization generates a large-scale background in which a central depression, due to the near-field couplings, is superimposed.

4.3.3 The 3-D NSOM image of metal coated tip

For the metal coated tip, the model is used as the same as non-coated dielectric tip except it coated with aluminum film of 25 nm (5 cells) and the height of tip of 350 nm (70 cells) shown in Fig.3(b). Figs. 6(a)-(d) show the calculated results in x-z sectional plane (at $y=70\phi$) and y- z sectional plane (at $x=70\Delta$) for p-polarization illumination and s-polarization illumination, respectively. The presence of a metal coating on the tip avoids lateral escape of light and significantly reduces the penetration of light emerging from the probe. The reflection light from the metallic layer of conic side couples with the incident light to form the high intensity standing wave and become maximum at the diameter of sectional plane in conic shape about 320 nm. Note that this diameter is different from the non-coated one (180nm).

Metals are good materials to confine the light wave in the tip since they have high absorption properties due to their high values in the imaginary part and negative dielectric constants. We choose Al as the coating film on probe surface. In Figs. 6(c) and 6(d), the incident wave is s-polarized, and penetrates inside the tip without any escape by the lateral surfaces. It propagates mostly forward to the apex, with an intense field emerging from the aperture. However, the field intensity produced by the very tip is weaker one yielded than a

non-coated tip. On the other hand, when considering the p-polarization illumination has shown in Fig. 6 (a) and (b), respectively, that the field intensity at the tip apex is not weak anymore. The higher intensity of fields are localized near the rim of tip aperture. It is well localized, and originates with the evanescent components were stopped before the tip end. Note the existence of a localized electric field enhancement at the edge along the rim of metal tip extending in teen nanometer range from the tip apex. The field enhancement of a metallic tip is originated mainly from the localized surface plasmon mode excited at the apex of the tip by the evanescent field.

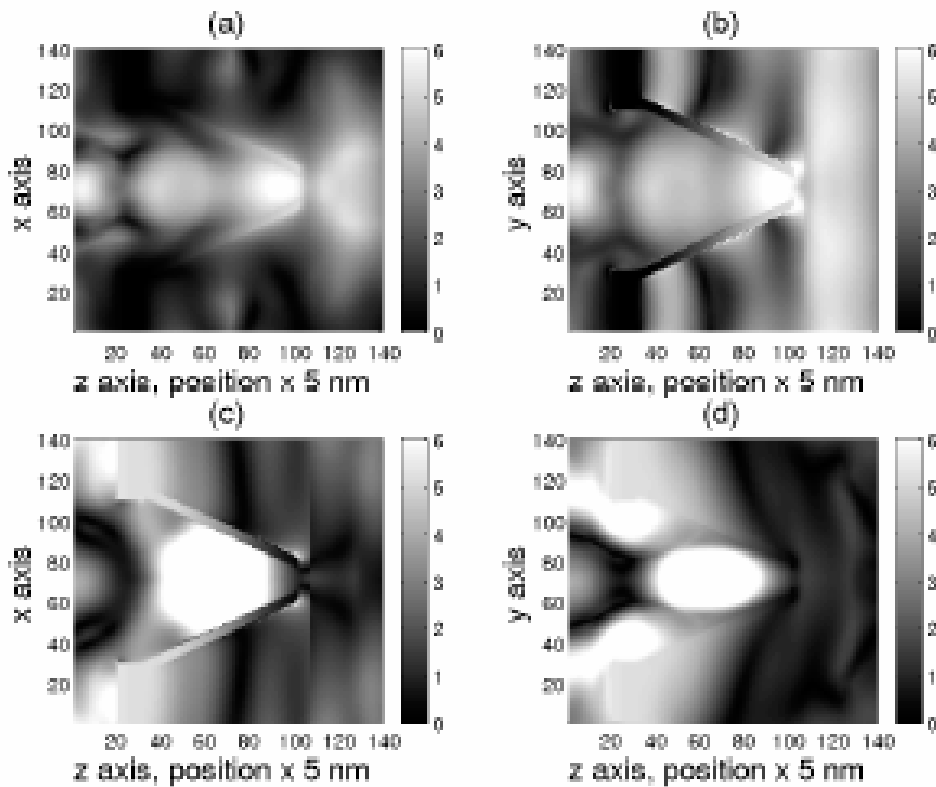


Fig. 4.6. Distribution of the 3-D electric field intensity modulus around the tip-sample coupling zone (metal coated tip): (a) in x-z plane (at $y=70 \text{ \AA}$), p-polarization, (b) in y-z plane (at $x=70 \text{ \AA}$), p-polarization, (c) in x-z plane (at $y=70 \text{ \AA}$), s-polarization, and (d) in y-z plane (at $x=70 \text{ \AA}$), s-polarization, respectively. The electric field results from an incident wave coming from the left side.

In addition, when the coating of a probe is very thin, such as less than 100 nm, the leakage of incident light should deteriorate the near-field signal in an experiment. The reasons why we still used the thinner film (25 nm) of coating are described as followed : (1) In our study, we are interested in the surface plasma around the rim of tip aperture. Plasmons may

play a role in the interaction of optical radiation with an aperture. In the near-field zone, the thinner of the metal coated probe is, the more the effects of surface atoms can play. Indeed, according to the frequency dependent dielectric properties, localized eigenmodes characterized by evanescent wavefunctions may be sustained by small objects and even by surfaces. If the thinner metal thin film is coated along the rim of tip apex, the aperture of tip can be looked as many dipoles at the symmetry positions around the circular aperture. The metal coated tip we used in Fig. 3(b) of the revised manuscript has an aperture opening of 50 nm at the apex of tip. If we choose the thickness of the coating of the probe larger than 100 nm, the effect of near-field is not obviously than the smaller one. (2) In order to gain a better understanding of plasmon excitation in near-field region, the shorter distance between tip and sample (30nm in this section), the smaller diameter of tip apex (50nm in this paper), and the thinner metal coating (25 nm in this paper) are needed in simulation domain. (3) Base on our simulations, we find that the different thickness of metal coating of a probe possess different cut-off plane inside the probe tip. The so-called cut-off plane which is a distinct plane between the radiation waves and evanescent field. The larger the thickness of coating is, the shorter the cut-off plane near the bottom side of the probe is. This is due to different boundary condition between the internal material (silica core) and the conic surface (Al thin film) of the probe. Besides, the thinner coating can be excited a larger number of surface plasmons which interact with the incident field and form the localized fields inside the probe tip. This is to be expected since many surface charge densities will be induced in this metal coating thin film by the incident electric fields.

4.3.4 Comparison of the 3-D NSOM image of dielectric tip and metal tip

Base on our simulations in this case of metal coated tip, the electric field decay rapidly along the transverse and longitudinal directions faster than the non-coated one(the results are not shown here). The depolarization phenomenon of electric field components is a near-field effect. The characteristics of edge enhancement of field intensity is declined as the distance from the tip apex increasing. For metal coated tip, this phenomenon exists several teen nanometer away from the tip aperture. Comparison with the field distribution decaying along z axis, the metal coated tip is faster than the non-coated one. For the metal coated one, the range of the field distribution decaying along z axis is about 40 nm at $1/e$ of maximum value and about 300 nm for the non-coated one. This is because of different waveguide structures and the different boundary conditions of tip apex. In the case of non-coated one, the HE_{11} can

propagate in any sizes of conic shapes. Since there is no clear cut-off plane to separate from the radiation wave and evanescent field. As regards to the coated one, the propagating mode has changed because of the existence of metal film and formed the near-field coupling into the forbidden zone. Upon the shielding effect of metal film, the presence of a metal coating on the tip avoids some lateral escape of light and concentrating the most of light inside the tip. It is well localized, and originates from evanescent components exclusively. Besides, the metal coated tip possess the phenomena of optical enhancement and beam confinement are due to the effect of surface atom in the region of nano dimension, i.e. the dipole polarization on the surface of aperture rim, and the beam blocking by the metal film of the conic surface.

In conclusion of this section, knowledge of the polarization is very important for the interpretation of images. The non-coated tip produce a well-confined and intense central spot from the s-polarization, with a central decay due to depolarization effects occurring in the p-polarization. For the metal coated tip, the p-polarization is responsible for the surface digging. As is shown in Figs. 6(a) and 6(b), respectively, the intensity of p-polarization is the most important one. In Figs. 6(c) and (d), we see that less light is generated by the tip apex in s-polarization. On the contrary, for p-polarization, there is a lot of light at the rim of aperture, coming from the metal coated and forming a local dipole along the rim of aperture.

4.3.5 A new design for fabricating an optimal tip

In this section, we present a new technique that combines a metal coated probe with a dielectric tip. Here we can adopt both the advantages of high transmission efficiency with no absorption of the dielectric tip and local enhancement of the metallic coating one (the tip coated with metallic thin film which could be used to produce spots smaller than that generated with the dielectric one) to design a new type of tip. We illustrate two kinds of improved tip which are named type A and type B in this section. The type A is a metal tip combines with the local dielectric one as shown in Fig.7(a). In the process of coating aluminum thin film of metal tip (by the evaporation process), we keep the tip apex exposed to fabricate local non-coated dielectric tip. That is to say, the tip bases on metal coated tip and extends the internal dielectric material outside the metal coated tip. The diameter of the tip apex is 50 nm (10 cells) and the length of non-coated part is 25 nm (5 cells). In front of the probe, at a distance of 15 nm (3 cells) a semi-infinite silicon medium was taken as the sample with the refractive index of $n=1.5$. The dimensions of each cell is $\Delta x=\Delta y =\Delta z =\Delta =5\text{nm}$, and the entire region model is $140(x) \times 140(y) \times 140(z)$ cells. The tip of type B is the same as

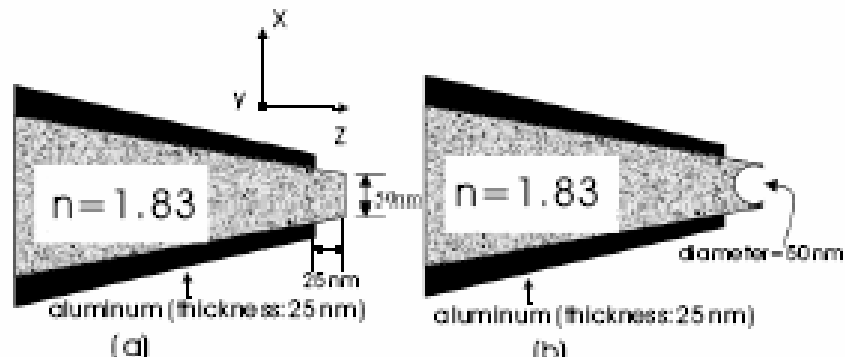


Fig. 4.7 Sectional plane diagram of 3-D improved tips: (a) the metal coated tip combines with the dielectric one, (b) the same as (a) except the hollow shape of tip apex formed a semi-spherical lens surface.

type except that a hollow shape of tip apex with radius of 25 nm formed a semi-spherical lens surface as shown in Fig. 7(b). Figs. 8(a)-(d), show the calculate results in x-z and y-z sectional lane by p-polarization illumination, respectively, where Fig.8(a) and (b) are corresponding to the tip of type A, Fig.8(c) and (d) are corresponding to the tip of type B. It can be seen in Fig. 8 (a) and (b) for the tip of type A, the light emerging from the top of metal coated part into the dielectric medium of the end of tip apex, it is expected that the optical transmission will be enhanced at the interface area between coated and non-coated part of tip apex. The field enhanced effect is due to the dipole polarization on the rim of metal aperture and the beam block by the metal layer (coated part). The high transmission effect at the top of tip apex is due to the effect of non-absorptive properties of dielectric medium (non-coated part). Because of the use of both metal coated part and non-coated part, the transmission light that illuminates from the tip apex will be excepted higher than that of a non-coated tip as shown in Fig.3 (a) and the spot size will be smaller than that metal coated one used alone as shown in Fig. 3(b), thus causing improved transmission and smaller spot size emerging from the tip apex. The spot size is about $200 \times 75nm^2$ as shown in Fig. 8(a) in x-z cross sectional plane for p-polarization illumination, which is smaller than that produced by the metal coated tip (about $300 \times 100nm^2$, as shown in Fig. 6(a), in x-z cross sectional plane for p-polarization illumination.). Note that the higher transmission will be observed. We can find the field intensity of spot size shown in the Fig. 8(b) is obviously higher than that shown in Fig. 6(b). The disadvantage of the tip of type A is a challenge for users to reach the accuracy requirements for fabricating a tip shown in Fig. 7(a).

As regards to the tip of type B, the light coming from the base of objective lens (the semi-spherical shape at the tip apex) which is focused the light on the output end of tip apex

in front of the sample surface. Because of the use of a semi-spherical lens shape at the tip apex shown in Fig. 7(b), the focus spot that illuminates from the hollow shape is expected smaller than that of a metal coated tip used alone as shown in Fig. 3(b), thus causing smaller spot size emerging from the tip apex. Owing to the small distance (in this case is 15nm) between tip and sample, a smaller spot is produced. The spot size will be reduced to $70 \times 30 \text{ nm}^2$ as shown in Fig. 8(c) in x-z cross sectional plane for p-polarization illumination case, which is much smaller than those produced by the tip of type A and metal coated tip used alone. Using the tip of type B, we can obtain a very small spot size of $70 \times 30 \text{ nm}^2$, which allows us to realized a recording density approximately of 300 Gb/in^2 . Besides, it is possible to reduce the recording marks below the laser beam spot by controlling the input beam power. The disadvantage of the tip of type B is the same as a challenge like the tip of type A, especially for fabricating process of a hollow shape on the tip apex shown in Fig. 7(b). Compares the intensity of field distribution between two improved tips (type A and type B) and metal coated tip used alone, Fig. 9 represents the intensity of field distribution along y axis direction, where dotted line represents the tip type A, solid line represents the tip of type B, and dashed line represents the metal coated tip used alone. It can be observed in Fig. 9, the tip of type A presents the stronger field intensity than the other two type of tips. That is to say, the smaller beam spot size by using the tip of type B is achieved at the expense of field intensity.

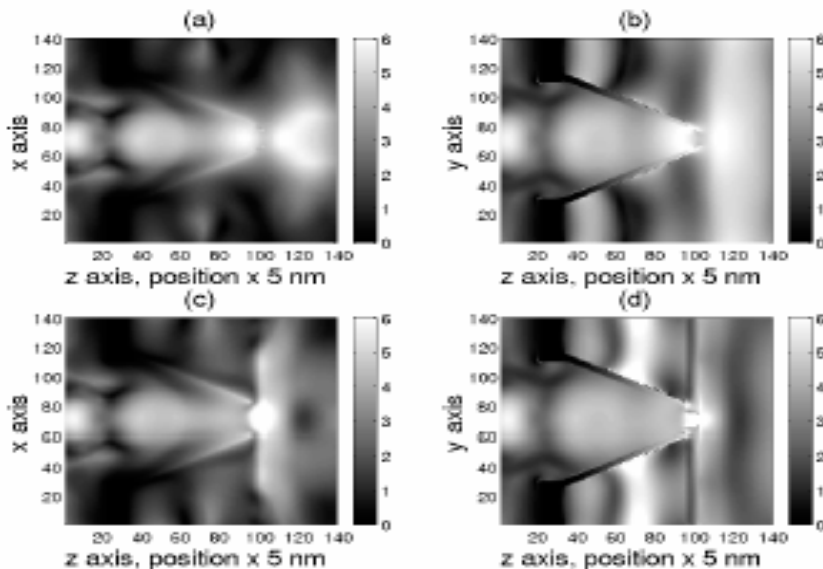


Fig. 4.8 Distribution of the 3-D electric field intensity modulus around the tip-sample coupling zone (improved tip) for p-polarization: (a)in x-z plane (at $y=70 \text{ nm}$), (b)in y-z plane (at $x=70 \text{ nm}$), (c)in x-z plane (at $y=70 \text{ nm}$), and (d)in y-z plane (at $x=70 \text{ nm}$), respectively. The electric field results from an incident wave coming from the left side.

By means of these simulation results, we can conclude that this two type of improved probes are better structures for our applications since they exhibit the advantages of both high throughput light efficiency and small beam spot size, and also the better type of tip pattern from the standpoint of fabrication process.

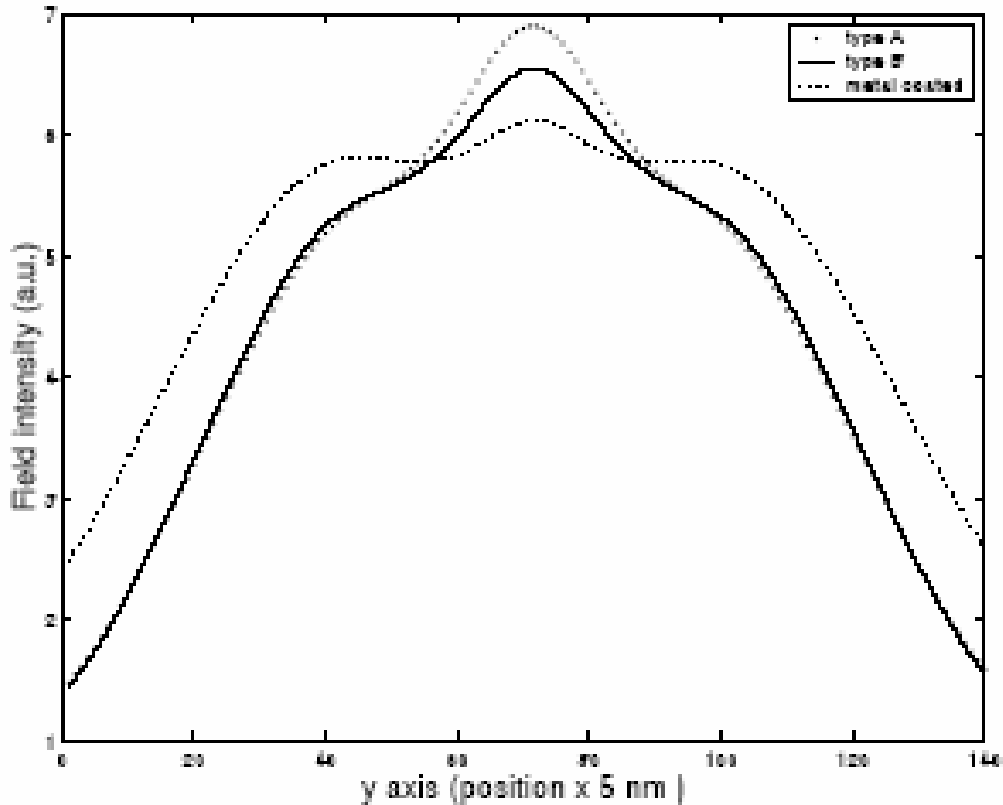


Fig. 4.9 Comparison of field intensity along y axis direction, where dotted line represents the tip of type A, solid line represents the tip of type B, and dashed line represents the metal coated tip used alone.

4.4. Conclusion

Near-field analysis has been studied to obtain more insight in the mechanisms responsible for NSOM architecture using the 3-D FDTD method. Among many types of structures simulated in this paper, including an aperture on an infinite metallic thin plate with and without sample interactions, comparisons of non-coated and coated tips, a novel probe structure combining metallic probe with local dielectric tip, a structure using a semi-spherical lens shape at the tip apex. In our simulations, we find some characteristics in 3-D NSOM structures are concluded in some details, which allows us to realize more clearly the physical mechanism in NSOM. Note that the depolarization phenomenon of electric field components is important in the near-field zone. The phenomena of optical enhancement and beam

confinement are due to the effect of surface atom in the region of nano dimension, i.e. the dipole polarization on the surface of aperture rim, and the beam blocking by the metal film of the conic surface. We have also verified the FDTD design of field enhancing NSOM probe that are experimentally feasible and provide a suggestion for fabricating an optimal probe. Using the improved tips with a tip size of 50 nm, we can get a very small spot size approximately the same dimensions as the diameter of tip apex, which are much smaller than those produced by the non-coated or metal coated tip used alone. In the near future, the non-linear response of the irradiated sample, the NSOM application using in photonic crystals will be further studied.

Reference

- [1] D.W. Pohl and D. Courjon, Eds., *NearField Optics*, NATO ASI Series E, Vol. 242 (Kluwer, Dordrecht, 1993)
- [2] E. Betzig, M. Isaacson and A. Lewis, *Appl. Phys. Lett.* 51(1987) 2088.
- [3] D.W. Pohl, W. Denk and M. Lanz, *Appl. Phys. Lett.* 44(1984) 651.
- [4] G. Krausch, S. Wegscheider, A. Kirsch, H. Bielefeldt, J.C. Meiners, J. Mlynek, *Opt. Commun.* 119(1995)283.
- [5] C. Girard and D. Courjon, *Phys. Rev. B* 42 (1990) 9340.
- [6] C.A. Brebbia, *The boundary element method for engineers* (Pentech Press, 1978).
- [7] Ch. Hafner, *The generalized multiple multipole technique for computational electromagnetics* (Artech, Boston, Mass., 1990).
- [8] L. Novotny, D.W. Pohl and P. Regli, *J. Opt. Soc. Am. A* 11 (1994)1768.
- [9] O.C. Zienkiewicz, and K. Morgan, *Finite element and approximation* (Wiley, 1983).
- [10] A. Castiaux, Ch. Girard, M. Spajer, S. Davy, *ultramicroscopy* 71(1998)49-58.
- [11] O.J.F. Martin, C. Girard, and A. Dereux, *Phys. Rev. Lett.* 74,526(1995).
- [12] K. S. Yee. *IEEE Trans. Antennas Propagat.*, 1966, AP-14:302-307.
- [13] A. Tadeu, *Computational Electrodynamics: The Finite-Difference Time-Domain Method*, Norwood, MA, Artech House, 1995.
- [14] K. S. Kunz and R. J. Luebbers, *The Finite Difference Time Domain Method for Electromagnetics*, Boca, Raton, FL, CRC Press, 1993
- [15] H. Furukawa and S. Kawata, *Opt. Commun.* 148,221(1998)
- [16] B. B. Akhremitchev, S. Pollack, and G. C. Walker, *Langmuir* 17,2774 (2001)
- [17] H. Nakamura, T. Sato, H. Kambe, K. Sawada, and T. Saiki, *J. Microsc.* 202, 66(2001)
- [18] J. L. Kann, T. D. Milster, F. Froehlich, R. W. Ziolkowski, AND J. Judkins, *Ultramicroscopy*, 57, 251 (1995)

- [19] D. Christensen, *Ultramicroscopy* 57, 189(1995)
- [20] R. G. Milner and D. Richards, *J. Microsc.* 202, 66(2001).
- [21] R.X. Bian, R.C. Dunn, X. S. Xie, and P. T. Leung, *Phys. Rev. Lett.* 75, 4772 (1995).
- [22] A. Roberts: *J. Appl. Phys.* 65 (1989) 2896
- [23] R. Chang, P.K. Wei, W.S. Fann, M. Hayashi and S.H. Lin : *J. Appl. Phys.* 81(1997) 3369
- [24] R. Muller and c. Lienau: *Appl. Phys. Lrft.* 76(2000) 3367
- [25] J. P. Berenger, *J. Comput. Phys.* 114, 185(1994).
- [26] C. Kittel, *Introduction to Solid-State Physics*, 6 th ed.(Wiley, New York ,1986).
- [27] R. Hummel, *Electronic Properties of Materials*(Springer, Berlin,1985).
- [28] J. Marvin, *CRC Handbook of Laser Science and Technology* (CRC, Cleveland, Ohio, 1986), Vol. 3, pp. 193-196.
- [29] R. J. Luebbers, F. Hunsberger, and K. S. Kunz, *IEEE Trans. Antennas Propag.* 39, 29 (1991).
- [30] J. B. Jukins and R. W. Ziolkowski:*J. Opt. Soc. Am. A* 12 (1995) 1974.
- [31] N. W. Ashcroft and N. D. Mermin, *Solid state Physics*(W. B. Saunder, Philadelphia, 1976).
- [32] J. H. Weaver et al., *Physics Data* 18(2) (1981) 71.
- [33] P. Drude, *Ann. Phys. (Leipzig)* 1, 566 (1990).
- [34] G. Mie, *Ann. Phys. (Leipzig)* 25, 377,1908.
- [35] P. W. Barber and S. C. Hill, *Light Scattering by Particles: Computational Methods* (World Scientific, Singapore, 1990).
- [36] M. Ohtsu:*IEEE J. Lightwave Technol.* 13(1995)1200.
- [37] R. Hummel, *Electronic Properties of Materials*(Springer, Berlin,1985).
- [38]G. Hass, in: *American InSTITUTE of Physics Handbook* (McGraw-Hill,New York,1972)pp. 6-125,ch. 6g.
- [39]H. Raether, *Suface plasmons on smooth and rough surfaces and on gratings*, Spinger, Berlin,1988.
- [40] M.Rudman, A. Lewis, A. Mallul, V. Haviv, I. Turovets, A. Shchemelinin, I. Nebenzahl, *J. Appl. Phys.* 79(1992) 4379.
- [41] J. Jersch, K. Dicjmann, *Appl. Phys. Lett.* 68(1996) 868.
- [42] B.D. Terris, H.J. Mamin, D. Rugar, *Appl. Phys. Lett.* 68(1996) 141.
- [43] P. J. Moyer, K. Walzer, M. Hietchold, *Appl. Phys. Lett.* 867(1995) 2129.
- [44] Hans U. Danzebrink, Annick Catstiaux, Christian Girard, Xavier Bouju, Gunter Wilkening,*Ultramicroscopy* 71 (1998) 371-377